Available online at www.sciencedirect.com
SCIENCE DIRECT®
Journal of Chromatography A, 1079 (2005) 287–298
JOURNAL OF CHROMATOGRAPHY A
www.elsevier.com/locate/chroma

Evaluation of multidimensional (ion-exchange/reversed-phase) protein separations using linear and step gradients in the first dimension

Kevin M. Millea [a], Ignatius J. Kass [b], Steven A. Cohen [b], Ira S. Krull [a], John C. Gebler [b], Scott J. Berger [b,*]

[a] *Department of Chemistry and Chemical Biology, Northeastern University, Boston, MA 02115, USA*
[b] *Life Sciences R&D, Waters Corporation, 34 Maple Street, Mail Stop: TG, Milford, MA 01749, USA*

Available online 13 May 2005

Abstract

The performance characteristics of multidimensional liquid chromatographic protein separations were evaluated using on-line electrospray mass detection, and a novel workflow for automated LC/MS data processing. Two-dimensional ion exchange/reversed-phase LC separations of *Escherichia coli* cytosol were conducted using either a continuous linear or discontinuous step gradient in the first dimension. Chromatographic profiles of the top 100 most abundant components were characterized to assess overall separation reproducibility within each mode, and to characterize differences in component distribution between the two modes of operation. Analysis of the resulting data indicates that multidimensional separations of complex protein mixtures can be done reproducibly. Furthermore, under the conditions employed within this study, a linear first dimension gradient was more effective at fractionating the protein mixture, distributing fewer major components to multiple second dimension cycles than an equivalent step gradient. The application of on line mass spectrometry, and automated processing of the resulting data, proved valuable for producing component level analysis of multidimensional protein separations.

Keywords: Multidimensional chromatography; Protein; LC/MS; Spectral deconvolution

1. Introduction

Liquid phase separations of intact proteins are becoming attractive alternatives to gel based separations as upfront fractionation techniques for the analysis of proteomic samples [1–3]. Liquid phase chromatographic or electrophoretic techniques permit a wide variety of separations mechanisms to be applied to intact protein separations, including molecular size [4], hydrophobicity [5], ionic character [6], and specific affinity interactions [7]. These methods offer an increased selectivity advantage over gel based methodologies, and can be easily scaled to meet sample or analysis requirements. They can also be applied to a variety of proteins (extreme p*I*, large/small, insoluble) that may not be compatible with gel based separations.

A second major advantage of liquid phase separations is that they are amenable to mass spectrometric detection, including direct coupling of the two techniques. When applied to intact proteins, mass spectrometric measurement accuracy can exceed that of gel based methods by several orders of magnitude. The intact mass of a protein represents the sum of the primary amino acid sequence, as well as all processing and modification events, and accurate mass determination can be used to fully characterize components within a complicated sample [8–11].

A wide variety of workflows employing liquid phase intact protein separations have been applied to the analysis of cellular machines and more complex proteomic mixtures. The characterization of 40S ribosomal subunit proteins, by a quadrupole LC/MS, was first reported by Louie et al. [5], while Galasinski et al. [12] applied a similar methodology to the analysis of histone proteins. Capillary LC coupled with Fourier transform ion cyclotron resonance mass spectrometry (FT-ICR-MS) was used by Lee et al. [8] to characterize intact yeast ribosomal proteins. In all these studies, meaningful information about co-translational processing and post-translational modification was obtained.

* Corresponding author. Tel.: +1 508 482 3592; fax: +1 508 482 3625.
E-mail address: Scott_Berger@waters.com (S.J. Berger).

0021-9673/$ – see front matter © 2005 Elsevier B.V. All rights reserved.
doi:10.1016/j.chroma.2005.04.048

Similar approaches have been applied to global proteomic studies. The Smith laboratory has analyzed cellular fractions from various microbes using the combination of capillary isoelectric focusing and FT-ICR-MS [13–16]. Reversed-phase liquid chromatography (RPLC) coupled with electrospray time-of-flight mass spectrometry (ESI-TOF-MS) was applied by Chong et al. [17] to develop protein molecular weight maps from premalignant and human cancer cell lines. These approaches provided a method for viewing overall differences in patterns of major protein components between samples.

Multidimensional separations that utilize orthogonal separation mechanisms offer improved separation capabilities over single dimension separations, and allow an increased number of components to be detected from complex mixtures. The basic theories on multidimensional separations provide that the resultant peak capacity of a two-dimensional (2D) separation can approach the product of the peak capacities of the individual dimensions [18–20]. The realization of this capacity requires the pairing of dimensions with sufficient selectivity differences to make efficient use of the increased separation space.

wide variety of multidimensional separation mechanisms have been coupled together to resolve complex protein mixtures, often in combination with on-line or off-line mass spectrometry. Chromatofocusing [6,21,22], size-exclusion [4,23,24], affinity [25], and ion-exchange chromatography [26,27] have all been used as a first dimension separation in combination with RPLC for online MS analysis of proteins. Free-flow electrophoretic–isoelectric focusing coupled with non-porous RPLC and ESI-TOF-MS detection has been used to examine the proteome of a human erythroleukemia cell line by Wall et al. [28,29]. Liu et al. [26], applied an integrated strong cation-exchange/reversed-phase (SCX/RPLC) 2D system with online MS detection to characterize yeast ribosomal extracts. Size-exclusion chromatography (SEC) followed by RPLC and MS detection was described by Nemeth-Cawley et al. [11]. In this study, the accurate mass determination of intact proteins using a quadrupole time-of-flight (Q-TOF) MS system permitted determination of component heterogeneity within an immunoglobulin fusion protein. Opiteck et al. have employed comprehensive multidimensional separations using both SEC/RPLC [30] and SCX/RPLC [31] systems combined with mass spectrometry for the characterization of intact proteins within an *Escherichia coli* cell lysate. These works illustrate the effectiveness of coupling multiple liquid phase separations with MS detection for the in depth characterization of protein samples.

In complex samples, chromatographic resolution of sample components is often insufficient to achieve baseline resolution of all species. Mass spectrometry is capable of detecting and characterizing co-eluting components, providing an additional effective dimension of separation. Analysis of resulting protein LC/MS datasets is complicated by the need to properly segment the data for summation and spectral deconvolution. In a sample of moderate complexity (the yeast ribosome, ~100 proteins), a multidimensional ion-exchange/reversed-phase (IEX/RP) separation was adequate to produce total ion chromatograms (TIC) with sufficient peak structure to permit automated peak identification, summation of spectra under the peaks, and production of a series of deconvoluted mass spectra for each identified peak [32]. As sample complexity increases, the TIC information becomes a less useful tool for analysis of LC/MS data, and time/scan based approaches become more valid. An analysis workflow of time based data segmentation, combined with spectral summation and deconvolution, was first applied to the analysis of the yeast large ribosomal subunit by Lee et al. [8]. We have developed a similar strategy where time based segmentation of spectra is combined with maximum entropy spectral deconvolution to produce deconvoluted mass versus retention time versus intensity maps of proteins from the LC/MS analysis of a complex mixture. This approach permits us to retain chromatographic profiles for each component, and evaluate the distribution of components throughout a multidimensional separation. The distribution (or dispersion) of a single component into multiple second dimension cycles has important consequences for both quantitative and qualitative aspects of the overall chromatographic separation.

In this work, we have evaluated the dispersion characteristics of cytosolic *E. coli* proteins subjected to multidimensional liquid chromatographic separations (MDLC), using MS detection as a tool to examine these separations at the component level. The approach permitted us to assess overall run-to-run variability, and evaluate two elution profiles (step versus linear) in the first dimension of separation. Creating the protein maps has also provided us with a basis for visualizing overall system performance, and for identification of characteristic patterns that differentiate chromatographic performance and component dispersion in both separation dimensions.

2. Experimental

2.1. Materials

All chemicals and reagents used were of analytical grade or higher. Buffers and salts were purchased from Sigma. Fisher OPTIMA brand acetonitrile (Fisher Scientific) and trifluoroacetic acid (TFA, Pierce) were used for RPLC. Purified water was generated in the laboratory using a Milli-Q purification system (Millipore).

2.2. Sample preparation

E. coli cytosol (50 mg/mL by a modified Bradford assay (Bio-Rad)) was prepared by a combination of French press cell lysis, and ultracentrifugation. The cytosol was diluted to a concentration of 12.5 mg/mL in 10 mM Tris (pH 8), aliquoted, and frozen until analyzed. Approximately 1250 μg of diluted cytosol was analyzed during each separation run.

2.3. Multidimensional LC configuration

System hardware, columns and software were obtained from Waters (Milford, MA, USA). An Alliance 2D Bioseparations System was applied for the multidimensional separation of *E. coli* cytosol. A 50 mm × 4.6 mm, 10 μm BioSuite Q-PEEK strong anion-exchange (SAX) column was used for the first separation dimension while the trapping of analytes from the SAX column was accomplished using two Symmetry300 C_4 10 mm × 2.1 mm, 3.5 μm columns. A Symmetry300 C_4 100 mm × 2.1 mm, 3.5 μm column was used for the reversed-phase second dimension separation. The overall system configuration, including the integrated valves used for multidimensional chromatography, is presented in Fig. 1. System control, data acquisition and data processing was accomplished using the MassLynx 4.0 software package running on a Windows XP based Pentium 4 computer system.

Within this integrated multidimensional analysis system (Fig. 1), the first dimension solvent delivery system controlled sample injection, and eluent composition for the SAX separation. The mobile phase in the first dimension was produced by an AutoBlend methodology [33], where solvent lines A (100 mM Tris–HCl) and B (100 mM Tris Base) controlled system pH at a constant buffer concentration, while solvent lines C (1.25 M NaCl) and D (Milli-Q water) were adjusted during a run to generate a step or linear salt gradient. A constant flow rate (0.3 mL/min) was maintained for the first dimension separation.

Flow from the SAX first dimension was alternately delivered to one of two trap columns through actuation of a 10-port, two-position, 2D column selection valve (Fig. 1). While one trapping column is in line with the first dimension, the other is placed in line with a second dimension binary solvent delivery system, and a single analytical reversed-phase column. This dual trap-single analytical column configuration was used for several reasons: (1) the trap column significantly reduces exposure of the analytical column to the damaging effects of the high salt and high pH mobile phase used in the first separation dimension; (2) the shorter trapping column required less washing time to remove nonvolatile salts, improving overall system cycle time; and (3) the lower back pressure of the trap column allowed the use of a high capacity (but pressure limited) porous SAX column in the first dimension.

Each time the first valve is actuated, a portion of first dimension eluent remains on the trap column now in line with the second dimension. This plug of material contains nonvolatile salts that can significantly degrade ESI-MS response and operation. To combat this effect, a second valve (Fig. 1, salt divert valve) was used to divert these materials from the trapping column to waste. Flow through this valve was directed to either to the mass spectrometer, or to waste through a backpressure regulator, which equalizes pressure between the analytical column and the waste stream. After a suitable desalting period (>20 column volumes), the second dimension flow was placed back in line with the analysis column, and components were eluted by a linear gradient of acetonitrile.

Flow from the second dimension was split nine to one, using a three-port tee fitting and static flow resistance, as

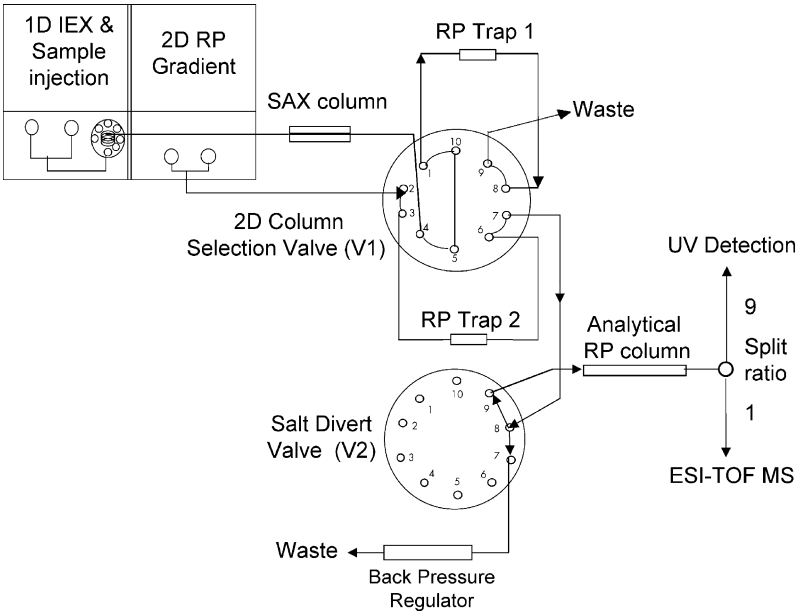

Fig. 1. System configuration for comprehensive multidimensional protein LC/MS analysis. A quaternary solvent delivery system (IEX pump) was used to control sample introduction and the first dimension chromatographic separation. An auxiliary binary solvent delivery module (RP pump) provided the second dimension eluent. The 2D column selection valve (V1) controlled flow from the first dimension to one of two alternating reversed-phase trap columns, and flow of second dimension eluent through the opposite trap, and an analytical column, for split analysis by UV and ESI-TOF-MS detection. Within this flow path a second valve (V2) acted to divert nonvolatile salts from the analytical column and detectors prior to initiation of the second dimension gradient.

measured under the initial gradient conditions. The splitting of second dimension effluent generated more optimal flow rates for MS analysis, and permitted additional detectors and/or fraction collection for the majority of column effluent.

2.4. Multidimensional LC system operation

The multidimensional LC system was evaluated using a 243 min, 0–500 mM NaCl gradient in the first dimension separation. In the first set of experiments this separation was accomplished using a continuous linear gradient (Fig. 2A). The linear gradient was divided into eight segments delivered to the second dimension trapping columns through timing of the 2D column selection valve (Fig. 1). In a second set of experiments, an equivalent discontinuous step gradient (eight steps of 62.5 mM NaCl, Fig. 2B) was applied. In both gradient modes, the anion-exchange columns were washed with 1000 mM NaCl to remove any remaining material, prior to restoring the system to initial conditions for the next run.

For each sampling segment of the linear and step gradients, the trapping columns were washed for 2 min (∼28 column volumes) before starting the second dimension gradient, and bringing the analytical column and mass spectrometer on line. The second dimension gradient (Table 1) was complex, starting with a an initial concentration of 10% acetonitrile in 0.1% formic acid and 0.005% trifluoroacetic acid, quickly rising to 30% organic, then a gradual increase to 55% organic over 20 min, before returning to initial conditions. Overall, this created a 29 min cycle in the second dimension. Flow rate in the second dimension was delivered at a rate of 0.5 mL/min, and both the trap and analytical columns were maintained at 30 °C.

System programming requirements introduced a one-cycle delay in the reversed-phase sampling of the linear gradient (Fig. 2A) compared to the step gradient. Thus, for the linear gradient, components that do not initially bind upon injection will be combined with those that elute from the first dimension during the first linear segment. This was the only expected difference between the two gradient modes, and was excluded from our analysis for purposes of direct comparison of the two modes of operation.

Table 1
Second dimension reversed phase gradient program

Reversed phase		Flow rate 500 μL/min	
Time (min)	E (%)	F (%)	Curve
0.00	90	10	1
2.00	70	30	6
22.00	45	55	6
23.00	45	55	6
25.00	90	10	6
27.00	90	10	6

E: water–0.1% formic acid–0.005% TFA and F: ACN–0.1% formic acid–0.005% TFA.

2.5. Mass spectrometry

A Micromass LCT ESI-TOF mass spectrometer (Waters) fitted with a Z-spray ion source was used for detection. A capillary voltage of 2850 V and a sample cone voltage of 35 V were used for data acquisition over a mass range of 700–3000 *m/z* while operating in the positive ion mode. Calibration was performed over a mass range of 300–3000 using a 0.4 mg/mL NaI solution. Calibration was confirmed by infusion of a 0.1 mg/mL horse heart myoglobin solution (mass 16 951.48 Da) with the specification of a deconvoluted mass accuracy of ±0.5 Da. An extended scan acquisition time of two seconds was applied to reduce the raw data file size of the 5.5 h run.

2.6. Data processing

Automated processing of LC/ESI-TOF-MS data was accomplished using a Visual Basic routine (Automated Maximum Entropy, or AutoME) developed in-house. Incremental segments of 10 MS spectra (20 s of retention time) were summed, then deconvoluted using MaxEnt1 deconvolution algorithm. The resulting deconvoluted spectrum for each of the various processing segments was centroided at unit resolution, thresholded at a global minimum intensity value of 40 counts, and output to a flat text file of retention time, mass, and intensity values. “2D Gel” (retention time, mass, intensity) and differential displays of this data were accomplished using the bubble plot feature of Microsoft Excel, and the ability to transparently overlay two bubble plots in Adobe Photoshop.

MaxEnt1 spectral deconvolution was done over the entire mass acquisition range (700–3000 *m/z*), using a uniform Gaussian damage model with a peak width at half height of 0.75 Da, an output mass range of 7000–40 000 Da, and an output resolution of 3 Da. A maximum of 10 iterations were done on the spectra to reduce overall computation time.

3. Results and discussion

3.1. Instrumental configuration and operation

An integrated multidimensional chromatographic system (Fig. 1), coupled with on-line ESI-TOF-MS detection was constructed as described in Section 2. An anion-exchange first dimension was coupled to a reversed-phase separation in the second dimension using automated valve switching that permitted capture of gradient segments or steps from the first dimension onto alternating trapping columns. In turn, these columns were placed in line with an analytical reversed-phase column, and introduced into an ESI-TOF MS detector. Results generated were in the form of intact protein LC/LC/MS data from the *E. coli* protein mixture.

In the course of these studies, two different gradient modes were examined for the first dimension of separation, while the same second dimension reversed-phase gradient cycle

(Table 1) was maintained for both separation formats. Overlays of the first and second dimension gradient profiles are shown as Fig. 2A (linear gradient) and Fig. 2B (discontinuous step gradient). In both modes, gradients of increasing ionic strength (0–500 mM NaCl) were applied over a 4 h separation.

3.2. Reproducibility of multidimensional LC/MS analyses at the component level

The reproducibility of multidimensional protein chromatographic separations is a fundamental question, which was addressed by examining chromatographic behavior of

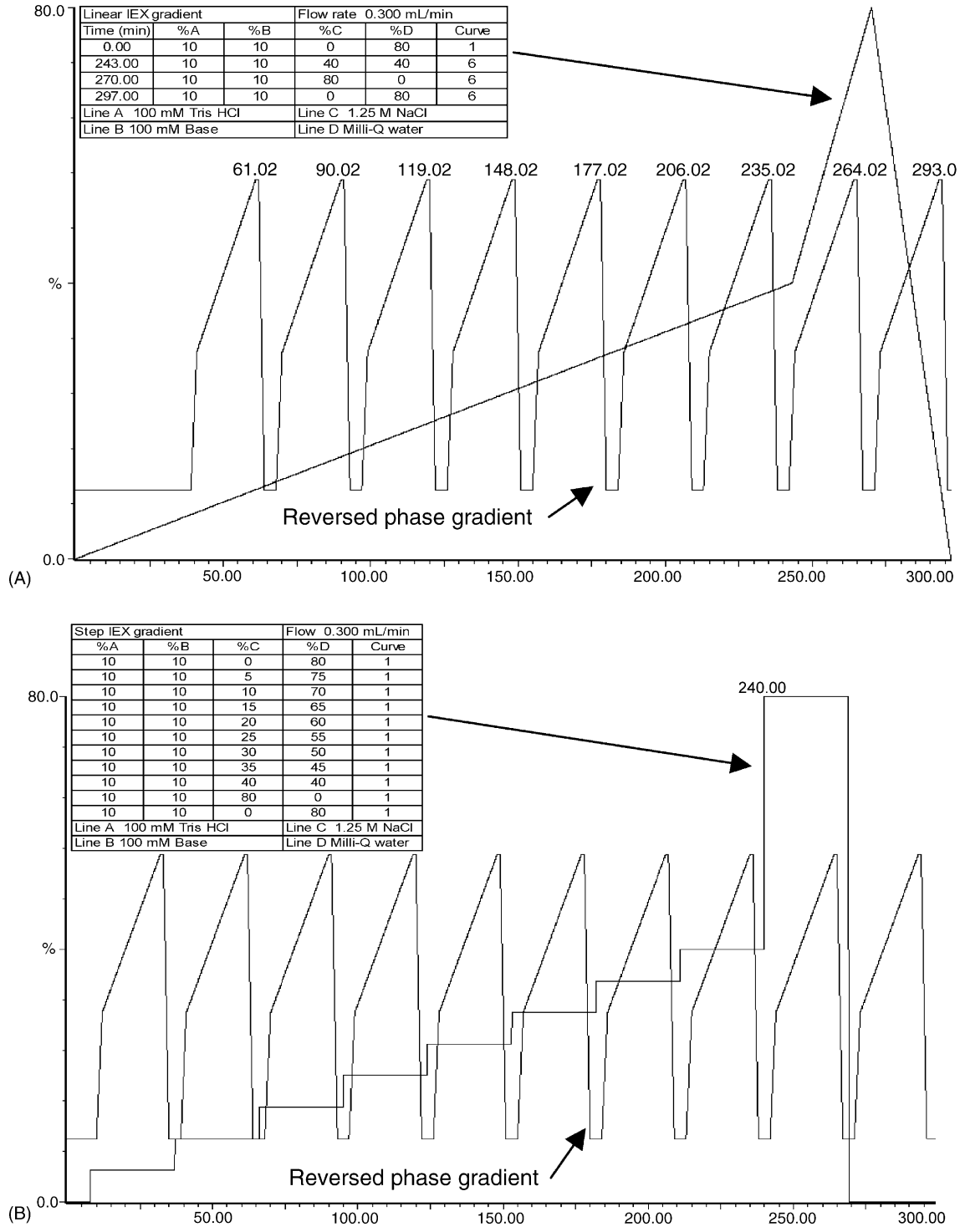

Fig. 2. Gradient profiles for multidimensional protein separations employing a linear (A) or step (B) gradient in the first dimension. The inset tables describe first dimension gradients programs for both gradient modes.

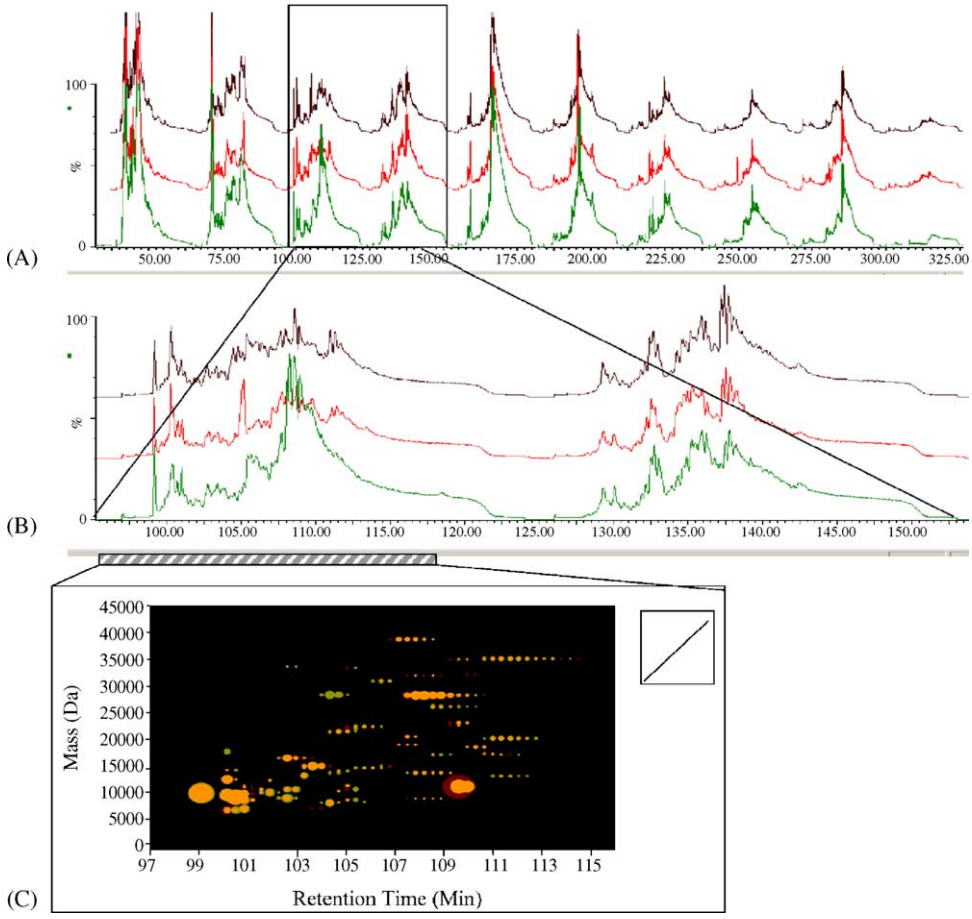

Fig. 3. Reproducibility of 2D (SAX/RP) LC/MS analysis of *E. coli* cytosol using a linear first dimension gradient. The TIC traces of three replicate analyses (A) are expanded (B) to show finer detail for the second dimension reversed-phase cycles. The first two LC/MS runs were processed to identify individual components within the earlier cycle, which are presented in a bubble plot map format (*x*-axis: retention time, *y*-axis: deconvoluted mass; bubble diameter: centroided intensity) of protein components. Components from the first run are shown in green, the second run in red, and overlapping components are shown in orange.

abundant species within a sample of *E. coli* cytosol. Experiments done previously (not shown) proved the MDLC/MS system capable of reproducibly separating an "ideal" protein mixture; however, proper behavior with complex protein mixtures could not be assumed. Proteomic mixtures contain a large number of chemically diverse proteins, present over a wide dynamic range, and constitute a serious challenge for obtaining reproducible separations. Changes in the physical properties of proteins, such as solubility, conformation, and sorbent interactions can vary over the course of multiple analyses, resulting in significant changes in chromatographic profiles of specific analytes during a separation, or between separations [34–36]. Specific and nonspecific protein–protein interactions also contribute to less reproducible chromatographic performance, as small differences in protein load may alter protein elution profiles [37–39].

E. coli cytosol (∼3000 potential proteins) was used to assess MDLC/MS separation reproducibility. Six injections of cytosol were made onto the system, and were resolved using step or linear gradients in the first dimension. Overlaid traces of the total ion chromatograms (TIC) of the six analyses are shown in Fig. 3A (linear gradient) and Fig. 4A (step gradient). General attributes observed in the TIC traces proved to be reproducible injection-to-injection for both gradient modes, while specific features, as seen in the expanded chromatogram views (Figs. 3B and 4B), were not quantitatively reproduced, demonstrating some run-to-run variations in both gradient modes.

Unlike analysis of simple protein mixtures, chromatographic performance is difficult to assess at the component level using the TIC chromatogram. Peaks within the TIC may have multiple components within them, making component quantitation based on TIC misleading. To identify individual components within each run, automated maximum entropy mass spectral deconvolution was applied to the LC/LC/MS data. This deconvolution workflow was performed within the MassLynx software package using a custom Visual Basic macro (Automated Maximum Entropy, or AutoME). This macro performed serial summation of 10 scan segments (corresponding to 20 s windows of retention time), followed by spectral deconvolution of the summed spectra using the MaxEnt1 deconvolution algorithm [32,40–44]. A segment size

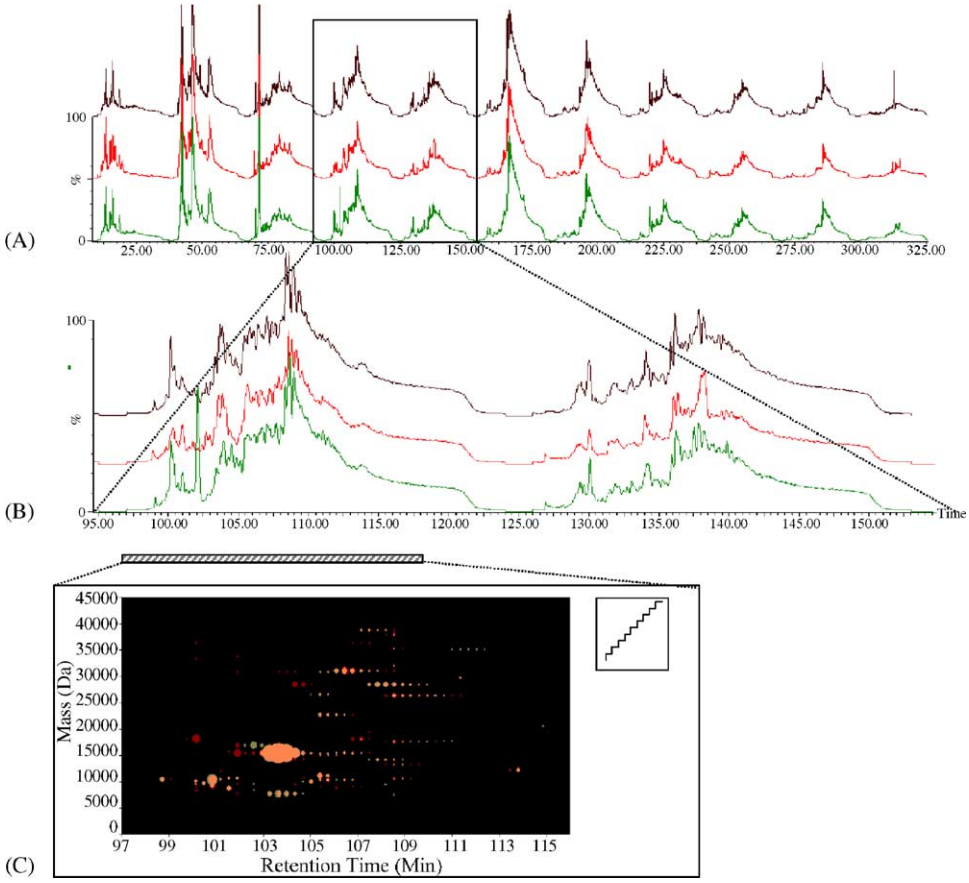

Fig. 4. Reproducibility of 2D (SAX/RP) LC/MS analysis of *E. coli* cytosol using a step first dimension gradient. The TIC traces of three replicate LC/MS analyses (A) are expanded (B) to show finer detail for the second dimension reversed-phase cycles. Two LC/MS runs were processed by the AutoME method to identify individual components within the earlier cycle, which are presented in a bubble plot map format (*x*-axis: retention time, *y*-axis: deconvoluted mass; bubble diameter: centroided intensity) of protein components. Components from the first run are shown in green, the second run in red, and overlapping components are shown in orange.

of 10 scans was utilized in order to retain chromatographic profile features for major components in the sample. Each deconvoluted spectrum was then centroided and thresholded, removing background noise and simplifying the data set. The end product of this AutoME process was a flat text file that contains a list of retention time, deconvoluted mass, and mass intensity values for all detected components.

This information was exported into Microsoft Excel and Adobe Photoshop to produce an overlay "mass map" of reversed-phase cycles corresponding to the same region (125–187 mM NaCl) in the first dimension separation for both gradient modes (Figs. 3C and 4C). Retention time (midpoint of the 10 scan segment) is plotted along the *x*-axis with deconvoluted mass plotted along the *y*-axis. Abundant components elute over multiple segments, and are displayed as a series of points along the retention time axis. The intensity of each component is represented by the diameter of the data point. In these displays, components detected in the first analysis run are shown in green, second analysis run in red, and those common to both are displayed in orange. Viewing these mass maps demonstrates the complexity of the sample, as multiple components (masses) can be observed co-eluting at any particular retention time. This observation demonstrates the utility (and additional dimensionality) of MS detection for analysis of complex mixtures, as it resolves components that otherwise would be observed as a single peak by methods such as UV–vis spectroscopy.

It is apparent that the large majority of components replicate between the two runs using both gradient modes, and most component intensities track well between runs. It can be seen in both modes that there are some components, unique to a single run that do not effectively replicate. This is expected for very low abundance components, where the paired signal may be subject to the applied noise thresholds, but the effect is also seen with several abundant components. It was established that these components appear to be unpaired, not because they are missing from one injection, but that their distribution has been somewhat altered between two analyses.

In order to give a more quantitative view of component detection reproducibility, the top 100 most intense masses (some obvious Na^+ and K^+ adducts of abundant compounds were removed) were compared across runs. In the linear gradient first dimension runs, approximately 10% of this mass

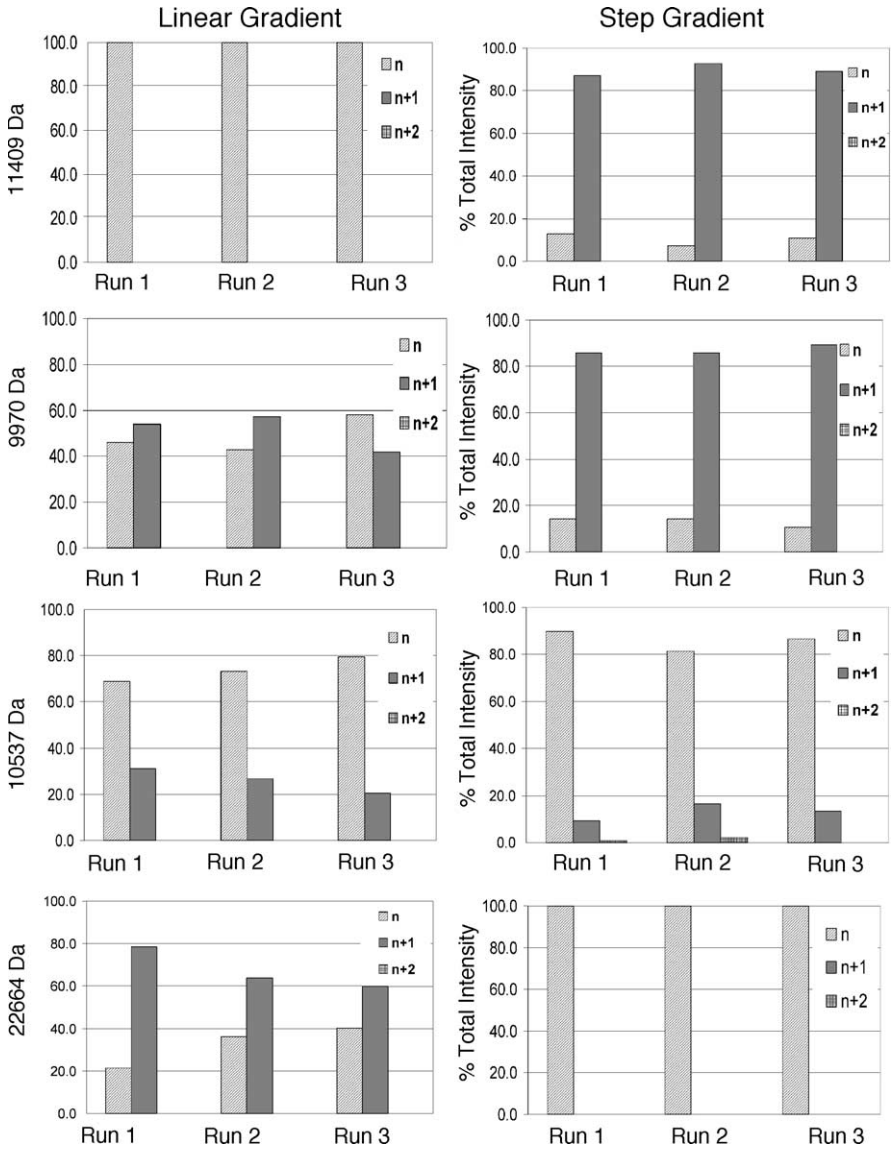

Fig. 5. Component distributions representative of first dimension peak splitting (dispersion into adjacent reversed-phase cycles). The distributions of four identified components (masses 11 049 Da, 9970 Da, 10 537 Da, and 22 664 Da) are shown as plots of the percent intensity of that component distributed over several reversed-phase cycles. Cycle n is the first cycle in which the component was detected, and $n+1$ would constitute the following reversed-phase cycle in the separation. Three replicate analyses are shown for each condition using both gradient modes. The first component (11 049 Da) illustrates splitting only in the step gradient mode, the next two (9970 Da and 10 537 Da) show splitting common to both modes, and the last (22 664 Da) shows splitting only for the linear mode.

list differed from run-to-run; however, all "missing" components were of lower abundance, and could be found at lower intensities in the suspect run. A slightly higher variation was seen in with step gradient runs, with approximately 14% of the top 100 most intense masses differing from run-to-run. This was also a result of thresholding effects, and all 100 components were reproducible between the runs when slightly lower abundance components were considered.

Combining the mass map and component list comparisons, we observe that while there can be small variations in the chromatographic profile and intensities of components observed during the multidimensional analyses, the overall approach is capable of reliably detecting the same components between sample replicates. The remaining sections of this work detail chromatographic behaviors of these abundant components, and describe observed run-to-run and method-to-method variations.

3.3. Analyte dispersion into multiple reversed-phase cycles

The optimal use of separation space within a multidimensional separation can be realized when each component produces a single chromatographic peak. This ideal situation can be achieved with simple protein mixtures, but is difficult to attain with real-world biological samples

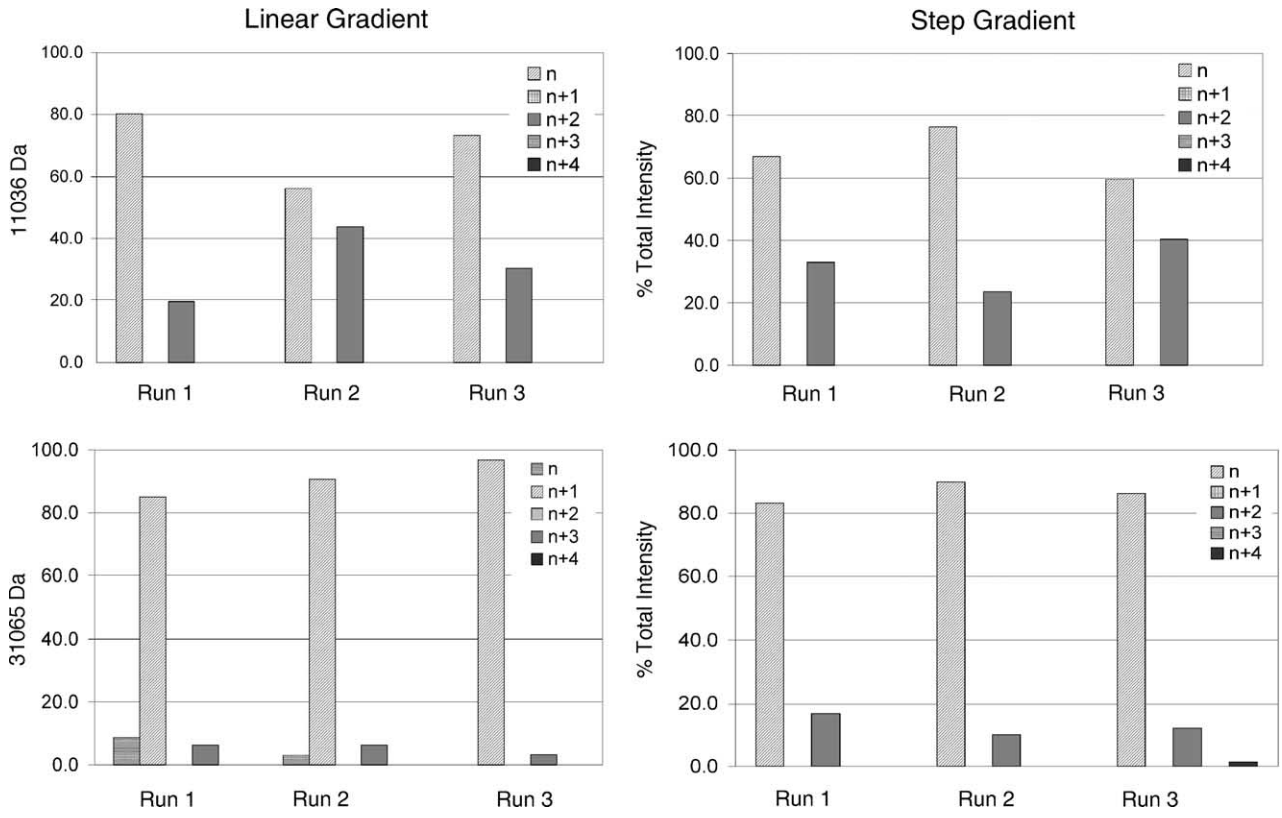

Fig. 6. Component distributions representative of second dimension peak carryover (dispersion into alternating reversed-phase cycles). The distributions of two identified components (masses 11 036 Da and 31 065 Da) are shown as plots of the percent intensity of that component distributed over several reversed-phase cycles. Cycle n is the first cycle in which the component was detected, $n+1$ would constitute the following reversed-phase cycle, and $n+2$ the next cycle in which the same trap column was developed. Three replicate analyses are shown for each condition using both gradient modes.

The system configuration used in these experiments (Fig. 1) made use of two trapping columns that alternated between sampling the first dimension separation and eluting trapped components onto the single analytical column, for second dimension LC/MS analysis. This configuration leads to dispersion of material into multiple reversed-phase cycles by several mechanisms: (1) the analyte may be carried over into two adjacent reversed-phase cycles (component splitting in first dimension); (2) the analyte may be carried into non-adjacent alternating reversed-phase cycles (second dimension trap column carryover); and (3) the analyte may be carried over into multiple continuous reversed-phase cycles (potential combination of both mechanisms).

The distribution of sample components, throughout the multidimensional protein separation, was investigated by examining the behavior of the top 100 abundant species common to both gradient formats. Identical masses with the same relative retention time in adjacent or in alternating reversed-phase gradients were determined to be characteristic of a first dimension or second dimension dispersion event. Individual component intensities for each reversed-phase cycle were produced by combining the intensity associated with that component over each AutoME processing segment in which it was observed. Total intensity for a component was calculated by combining component intensity over all reversed-phase cycles where the component was identified. Figs. 5–7 provide representative examples of component dispersion in the first, second, or both separation dimensions. In these figures, component distributions are plotted as percent of the total component intensity detected in an initial second dimension RP cycle (n) and subsequent cycles ($n+1$, $n+2$ etc.).

3.3.1. Dispersion of analyte into adjacent reversed-phase cycles-dispersion in the first separation dimension

The stoichiometric displacement model for ion-exchange chromatography of proteins argues that analytes are cooperatively retained on column by multiple points of ionic interaction between protein and sorbent. The effective number of interaction points within a particular protein is variable, and will be affected by a number of factors, including: protein conformation, system pH, steric factors, protein loading, and protein–protein interactions [34,35,38,45–47]. In practice, the theory predicts that proteins will have negligible linear velocity, until a critical eluent strength is reached, and then there will be an abrupt change to maximal linear velocity. Thus, a step gradient could potentially be more effective in cleanly resolving proteins than an equivalent linear gradient, sampled at the same interval, assuming a protein has uniform interactions within the chromatographic system.

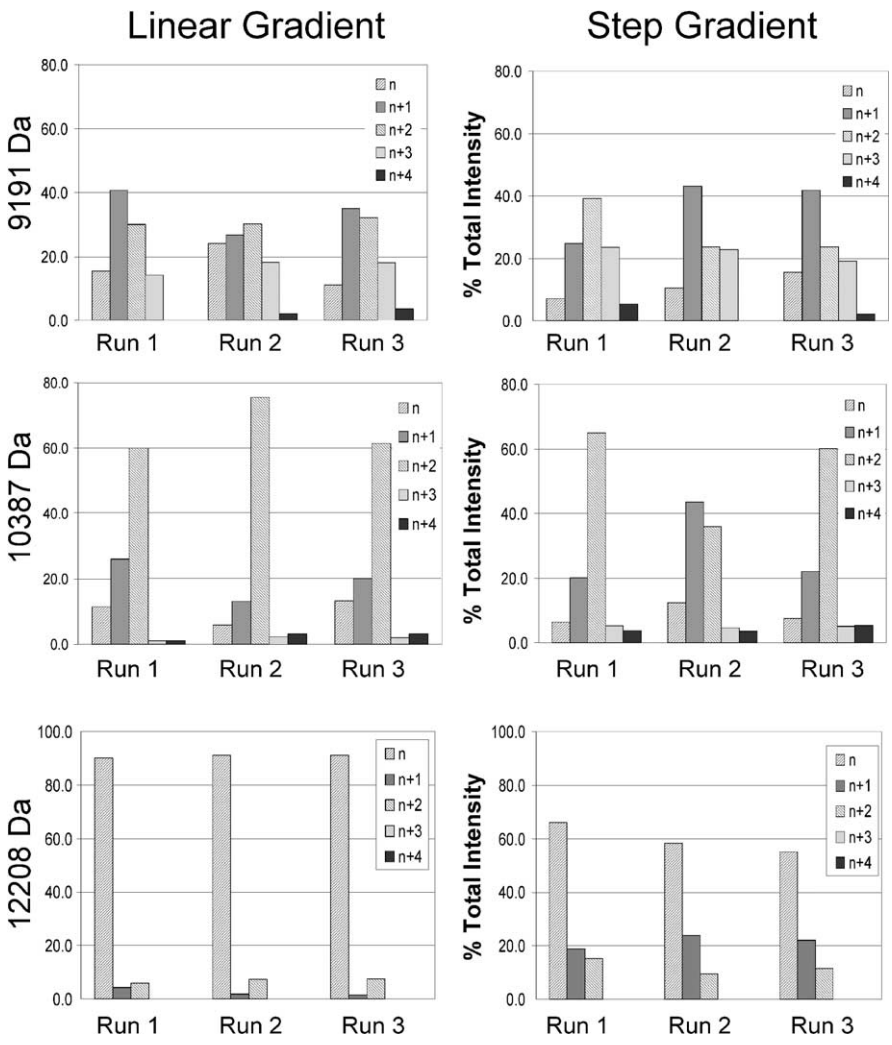

Fig. 7. Component distributions representative of component dispersion in multiple dimensions (dispersion into multiple adjacent reversed-phase cycles). The distributions of three identified components (masses 9191 Da, 10 387 Da, and 12 208 Da) are shown as plots of the percent intensity of that component distributed over several reversed-phase cycles. Cycle n is the first cycle in which the component was detected; subsequent cycles are identified as $n+1$, $n+2$, $n+3$, etc. Three replicate analyses are shown for each condition using both gradient modes.

In the linear gradient mode, the first dimension is physically sampled by the second dimension by actuation of the 2D column select valve (Fig. 1), and components eluting during this switching event will be split between two adjacent reversed-phase cycles. A representative example of a component that exhibits such first dimension splitting is presented within Fig. 5 (mass 22 664 Da). While observed in both gradient modes, our data indicate that the majority of first dimension peak splitting cases occurred only in the step mode (Fig. 5 mass 11 049 Da), or in both modes (Fig. 5, masses 9970 Da and 10 537 Da).

First dimension peak splitting was observed to be generally reproducible (±15%) as seen from the intensity profiles of the replicate analyses presented in Fig. 5. The overall data indicate that components were effectively resolved into the same reversed-phase cycles run-to-run, but that small changes in the relative distribution of components between the cycles contributed the larger source of variation.

Peak splitting is not just a chromatographic phenomenon, but may describe an underlying heterogeneity of a protein's structure. Protein structure is not static, but rather dynamic, and a protein can sample a variety of conformations depending on the surrounding environment. The use of denaturing conditions may produce more homogeneity of protein–sorbent interactions, but also requires the use of additional agents to maintain protein solubility, and prevent large-scale secondary chromatographic effects due to the exposure of hydrophobic core regions of proteins. While this parameter is outside the scope of this work, the utility of exploring such denaturing conditions to reduce first dimension dispersion is warranted.

3.3.2. Dispersion into alternating reversed-phase cycles—second dimension carryover events

Dispersion into alternating reversed-phase cycles, n, $n+2$, $n+4$, etc. with little or no material in the $n+1$ cycle, can be

attributed to classical "carryover" or "ghosting" phenomena in the second dimension. We observe multiple instances where incomplete elution of material off a trapping column is apparent, and a component signal is observed the next cycle in which that trap column is employed. Representative examples of dispersion in alternating reversed-phase cycles (n and $n+2$) are shown in Fig. 6 (masses 11 036 Da and 31 065 Da). In some instances the analyte is also seen in a third reversed-phase cycle (e.g. mass 31 065 Da) that is $n+4$ cycles away from the first appearance in the separation.

While component separations in the second dimension cannot be fully independent of first dimension behaviors, the given examples (Fig. 6) are representative in showing that the reversed-phase behavior of a component plays the primary role in determining second dimension component dispersion. While we observe that analyte hydrophobicity and intensity do not directly correlate with second dimension carryover, intense components were more likely to display this phenomenon.

3.3.3. Carryover into multiple continuous reversed-phase cycles—complex dispersion patterns

Dispersion of analytes into multiple adjacent reversed-phase cycles may be attributed to the combination of first and second dimension dispersion events. However, using the current chromatographic configuration, it is difficult to differentiate components that are grossly dispersed in the first dimension from those that experience problems in both dimensions. One characteristic pattern (Fig. 7, mass 12 208 Da, linear) that may help differentiate these behaviors is that an alternating high/low intensity pattern would likely be representative of stronger dispersion contributions from the second dimension separation. Most components that show multiple cycle dispersion do not exhibit this particular dispersion pattern, but rather more of an apex pattern indicative of extensive first dimension dispersion (Fig. 7, masses 9191 Da and 10 387 Da). Those components that did show extensive dispersion behavior into multiple reversed-phase cycles displayed this behavior in both the step and linear gradient first dimension formats. Such components show reproducible patterns of elution run-to-run, but exhibit the greatest intensity variations of the three component dispersion mechanisms.

3.3.4. Overall component distributions

To assess overall behaviors of components between the two gradient modes, the top 100 most intense analytes were characterized with respect to first and second dimension chromatographic performance. The Venn intersections of this analysis are presented as Fig. 8. The data (component RP distributions in duplicates runs of both gradient modes) underlying this analysis have been made available as a supplementary data file in a Microsoft Excel format. Approximately half (51 of 100) of the components exhibit some type of dispersive behavior during the multidimensional separation. Of these 51 components, 28 were observed to exhibit a dispersive behavior (but not necessarily the identical type of behavior) with both step and linear first dimension gradient modes, 21 were observed to have dispersive behavior in only the step gradient separation, and only 2 components had shown dispersion unique to the linear gradient mode. Dispersion of the two components unique to the linear mode appears to arise from actuation of the second dimension column selection valve during component elution, and resulting first dimensional peak splitting.

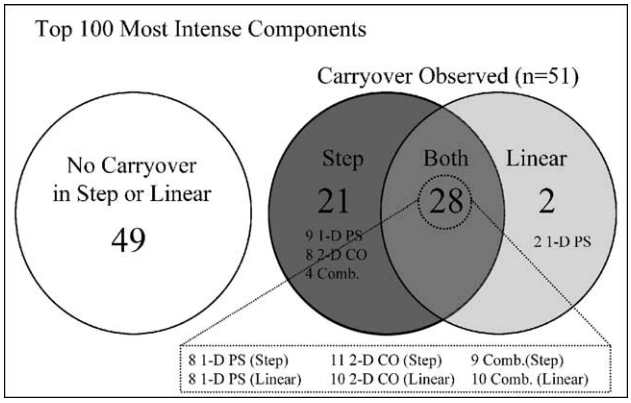

Fig. 8. Venn diagram describing the dispersion of the top 100 of the most intense components. The distribution of chromatographic dispersion events for the top 100 most abundant components (both gradient modes) is presented. More detailed information is provided on the nature of dispersion, where 1D PS represents the first dimension peak splitting, 2D CO the second dimension carryover and Comb. the combined first and second dimension dispersion effects.

The dispersive behavior of those components unique to step mode, and common to both gradient modes, is derived from roughly equal contributions of first and second dimension chromatography (Fig. 8). Overall, using the current experimental conditions, the linear gradient used for the first dimension anion-exchange separation was more effective at minimizing dispersion events, when compared to step gradient elution.

4. Conclusions

In this work, we have demonstrated a component-level approach for the evaluation of multidimensional protein separations using on line ESI-TOF-MS detection. A novel automated spectral deconvolution routine (AutoME) was employed to identify chromatographic profiles of individual components eluting during multidimensional LC/MS separations. We have applied this methodology to illustrate differences between MDLC separation modes, where linear and step gradients were used for the first dimension separation. This approach provided an effective tool for demonstrating run-to-run separation reproducibility within each mode, as well as revealing differences in chromatographic effectiveness between the two separation modes.

Overall, half of all abundant *E. coli* proteins behaved ideally, yielding a single peak for each detected mass. Using a common set of system conditions, it was determined that

sampling of a linear first dimension gradient distributed fewer major components to multiple reversed-phase cycles than an equivalent step gradient. Furthermore, it can be clearly shown with our data, that chromatographic dispersion of sample components is due to contributions from both separation dimensions, providing multiple avenues for optimizing this separation method.

Going forward, we now have a benchmark, and an analytical tool, to systematically test changes to chromatographic hardware, separations chemistries, and separation strategies that can be applied to the analysis of a complex sample. In particular, the evaluation of denaturants, surfactants, buffers/pH, salts, reduction/alkylation, and separation temperatures should provide critical insights for obtaining optimal protein separations for global proteomic analysis.

Appendix A. Supplementary data

Supplementary data associated with this article can be found, in the online version, at doi:10.1016/j.chroma.2005.04.048.

References

[1] H. Wang, S. Hanash, J. Chromatogr. B 787 (2003) 11.
[2] T. Wehr, LC–GC North Am. 20 (2002) 954.
[3] K.M. Millea, I.S. Krull, J. Liq. Chromatogr. Relat. Technol. 26 (2003) 2195.
[4] G.J. Opiteck, S.M. Ramirez, J.W. Jorgenson, M.A. Moseley III, Anal. Biochem. 258 (1998) 349.
[5] D.F. Louie, K.A. Resing, T.S. Lewis, N.G. Ahn, J. Biol. Chem. 271 (1996) 28189.
[6] D.M. Lubman, M.T. Kachman, H. Wang, S. Gong, F. Yan, R.L. Hamler, K.A. O'Neil, K. Zhu, N.S. Buchanan, T.J. Barder, J. Chromatogr. B 782 (2002) 183.
[7] S. Kishino, K. Miyazaki, J. Chromatogr. B 699 (1997) 371.
[8] S.W. Lee, S.J. Berger, S. Martinovic, L. Pasa-Tolic, G.A. Anderson, Y. Shen, R. Zhao, R.D. Smith, Proc. Natl. Acad. Sci. U.S.A. 99 (2002) 5942.
[9] G.E. Reid, S.A. McLuckey, J. Mass. Spectrom. 37 (2002) 663.
[10] J.R. Hayter, D.H. Robertson, S.J. Gaskell, R.J. Beynon, Mol. Cell Proteomics 2 (2003) 85.
[11] J.F. Nemeth-Cawley, B.S. Tangarone, J.C. Rouse, J. Proteome Res. 2 (2003) 495.
[12] S.C. Galasinski, K.A. Resing, N.G. Ahn, Methods 31 (2003) 3.
[13] Y. Shen, S.J. Berger, R.D. Smith, J. Chromatogr. A 914 (2001) 257.
[14] R.D. Smith, L. Pasa-Tolic, M.S. Lipton, P.K. Jensen, G.A. Anderson, Y. Shen, T.P. Conrads, H.R. Udseth, R. Harkewicz, M.E. Belov, C. Masselon, T.D. Veenstra, Electrophoresis 22 (2001) 1652.
[15] P.K. Jensen, L. Pasa-Tolic, G.A. Anderson, J.A. Horner, M.S. Lipton, J.E. Bruce, R.D. Smith, Anal. Chem. 71 (1999) 2076.
[16] P.K. Jensen, L. Pasa-Tolic, K.K. Peden, S. Martinovic, M.S. Lipton, G.A. Anderson, N. Tolic, K.K. Wong, R.D. Smith, Electrophoresis 21 (2000) 1372.
[17] B.E. Chong, R.L. Hamler, D.M. Lubman, S.P. Ethier, A.J. Rosenspire, F.R. Miller, Anal. Chem. 73 (2001) 1219.
[18] J.C. Giddings, Anal. Chem. 56 (1984) 1258A.
[19] R.E. Murphy, M.R. Schure, J.P. Foley, Anal. Chem. 70 (1998) 1585.
[20] A. Malik, in: L. Mondello, A.C. Lewis, K.D. Bartle (Eds.), Multidimensional Chromatography, Wiley, West Sussex, UK, 2002.
[21] S. Zheng, K.A. Schneider, T.J. Barder, D.M. Lubman, BioTechniques 35 (2003) 1202.
[22] K. Zhu, M.T. Kachman, F.R. Miller, D.M. Lubman, R. Zand, J. Chromatogr. A 1053 (2004) 133.
[23] A.V. Lemmo, J.W. Jorgenson, J. Chromatogr. 633 (1993) 213.
[24] Z. Zhang, D.L. Smith, J.B. Smith, Proteomics 1 (2001) 1001.
[25] J. le Coutre, J.P. Whitelegge, A. Gross, E. Turk, E.M. Wright, H.R. Kaback, K.F. Faull, Biochemistry 39 (2000) 4237.
[26] H. Liu, S.J. Berger, A.B. Chakraborty, R.S. Plumb, S.A. Cohen, J. Chromatogr. B 782 (2002) 267.
[27] B. Feng, A.H. Patel, P.M. Keller, J.R. Slemmon, Rapid Commun. Mass Spectrom. 15 (2001) 821.
[28] D.B. Wall, M.T. Kachman, S. Gong, R. Hinderer, S. Parus, D.E. Misek, S.M. Hanash, D.M. Lubman, Anal. Chem. 72 (2000) 1099.
[29] D.B. Wall, M.T. Kachman, S.S. Gong, S.J. Parus, M.W. Long, D.M. Lubman, Rapid Commun. Mass Spectrom. 15 (2001) 1649.
[30] G.J. Opiteck, J.W. Jorgenson, R.J. Anderegg, Anal. Chem. 69 (1997) 2283.
[31] G.J. Opiteck, K.C. Lewis, J.W. Jorgenson, R.J. Anderegg, Anal. Chem. 69 (1997) 1518.
[32] A.G. Ferrige, M.J. Seddon, J. Skilling, N. Ordsmith, Rapid Commun. Mass Spectrom. 6 (1992) 765.
[33] W. Warren, A. Peterson, T. Wheat, Am. Biotechnol. Lab. 7 (1989) 34.
[34] F.E. Regnier, Science 238 (1987) 319.
[35] W. Kopaciewicz, M.A. Rounds, J. Fausnaugh, F.E. Regnier, J. Chromatogr. 266 (1983) 3.
[36] X. Geng, F.E. Regnier, J. Chromatogr. 296 (1984) 15.
[37] E. Karlsson, L. Ryden, J. Brewer, Protein Purification; Principles, High-Resolution Methods, in: and Applications, second ed., Wiley-VCH, New York, 1998.
[38] W. Xu, F.E. Regnier, J. Chromatogr. A 828 (1998) 357.
[39] R.K. Scopes, Protein Purification; Principles and Practice, third ed., Springer, New York, 1994.
[40] A.G. Ferrige, M.J. Seddon, B.N. Green, S.A. Jarvis, J. Skilling, Rapid Commun. Mass Spectrom. 6 (1992) 707.
[41] D.M. Horn, R.A. Zubarev, F.W. McLafferty, J. Am. Soc. Mass Spectrom. 11 (2000) 320.
[42] J. Skilling, Classic Maximum Entropy, Kluwer, Norwell, MA, 1989.
[43] Z. Zhang, A.G. Marshall, J. Am. Soc. Mass Spectrom. 9 (1998) 225.
[44] H. Zheng, P.C. Ojha, S. McClean, N.D. Black, J.G. Hughes, C. Shaw, Rapid Commun. Mass Spectrom. 17 (2003) 429.
[45] R.R. Drager, F.E. Regnier, J. Chromatogr. 359 (1986) 147.
[46] C.K. Ratnayake, F.E. Regnier, J. Chromatogr. A 743 (1996) 25.
[47] I. Mazsaroff, L. Varady, G.A. Mouchawar, F.E. Regnier, J. Chromatogr. 499 (1990) 63.